

## Article

# Numerical Method for Creep Analysis of Strengthened Fatigue-Damaged Concrete Beams

Yunfei Ding <sup>1,2</sup>, Yan Fang <sup>3</sup>, Weiliang Jin <sup>3</sup>, Jun Zhang <sup>4</sup> , Bixiong Li <sup>1</sup> and Jianghong Mao <sup>1,\*</sup> <sup>1</sup> College of Architecture and Environment, Sichuan University, Chengdu 610065, China<sup>2</sup> School of Civil Engineering, Henan University of Technology, Zhengzhou 450001, China<sup>3</sup> Institute of Structural Engineering, Zhejiang University, Hangzhou 310085, China<sup>4</sup> College of Civil Engineering and Architecture, Ningbo Tech University, Ningbo 315100, China

\* Correspondence: jhmao@scu.edu.cn

**Abstract:** Fatigue-damaged concrete improves the load-bearing capacity of components by increasing the cross section. However, the creep performance of damaged components after the repair has received less attention. Thus, this study establishes a constitutive creep model of strengthened fatigue-damaged concrete on the basis of damage mechanics and numerically simulates the strengthened component. The accuracy of the proposed model is verified by conducting creep tests on fatigue-damaged concrete beams. According to the numerical simulation results, increasing the section height profoundly affects the ability to control their creep deflection. The incremental creep deflection of the beams with a strengthened section height of 50, 100, and 150 mm loaded for 365 days decreased by 0.107, 0.228, and 0.326 mm, respectively, compared with the unstrengthened damaged beam. Moreover, this reinforcement method excellently controls the deflection of the damaged components under a negative bending moment. The model can forecast the creep deformation of undamaged components or damaged components after being strengthened, which facilitates structural maintenance and decision-making about reinforcement.



**Citation:** Ding, Y.; Fang, Y.; Jin, W.; Zhang, J.; Li, B.; Mao, J. Numerical Method for Creep Analysis of Strengthened Fatigue-Damaged Concrete Beams. *Buildings* **2023**, *13*, 968. <https://doi.org/10.3390/buildings13040968>

Academic Editors: Jong Wan Hu, Junwon Seo and Andreas Lampropoulos

Received: 31 January 2023

Revised: 30 March 2023

Accepted: 1 April 2023

Published: 6 April 2023



**Copyright:** © 2023 by the authors. Licensee MDPI, Basel, Switzerland. This article is an open access article distributed under the terms and conditions of the Creative Commons Attribution (CC BY) license (<https://creativecommons.org/licenses/by/4.0/>).

**Keywords:** structural reinforcement; fatigue; creep; deflection; numerical simulation

## 1. Introduction

Fatigue and creep of concrete structures are specific time-varying properties during the entire life cycle of engineering structures, primarily studied independently [1], with less coupled consideration. The fatigue damage phenomenon is evident in pier and bridge projects, which are often strengthened by increasing the cross section. Because of the difference between the creep coefficients of new and old concrete after reinforcement, the deflection of the components is continuously increasing. This phenomenon has been confirmed in the related literature [2–4]. Due to the effect of fatigue damage, the deflection and stress redistribution of strengthened components may be severe. Therefore, studying the long-term deformation of strengthened fatigue-damaged components is crucial and valuable. The mechanism for the long-term deformation can be analyzed in terms of the micro-difference in the creep of new and old concrete and the degree of fatigue damage.

The long-term performance of concrete components strengthened by the increased cross section method was first noticed in the 1980s [5,6]. Wang et al. investigated the effect of the shrinkage and creep on prestressed new–old concrete composite beams experimentally and revealed that the concrete strain, deflection, and section curvature along the beam height increased gradually with time [7]. In engineering, increasing the cross section is often used to improve the structural bearing capacity and stiffness, so it is essential to identify the effect of increasing the cross section on the creep of components. Yang et al. considered deformation coordination as a calculation condition and presented the influence of shrinkage and creep by introducing the cross section cooperative work coefficient into the classical calculation formula for concrete structure design [8]. Other works have reported

on the creep of composite structures due to the significant influence of steel on the creep development of concrete materials [9–12]. Fang et al. proposed a method to calculate the midspan deflection and cross-sectional stress of composite beams under shrinkage and creep on the basis of the average curvature method [13].

The above studies do not consider the influence of damage to strengthened beams [14,15], although they are often damaged. Damage affects the creep of concrete materials and components [14,15]. The study by Farah, M., et al. showed a drop in Young's modulus and residual strength after creep loadings in partially damaged beams, implying the development of a state of weakness in beams subjected to an increasing creep load [16]. Cao et al. studied concrete creep under corrosion and load coupling in a solution environment and found that the creep of columns increased with steel corrosion. When the reinforcement ratio is low, the creep coefficient of early-age concrete under corrosion and load coupling is lower than that of late-age concrete [17]. Different from the above studies, the research on the creep problem of strengthened damaged members includes not only the creep micro-difference between old and new concrete but also the effect of initial damage on the creep of the components. As far as this problem is concerned, few relevant literature reports exist. However, structures such as bridges and piers are often subjected to heavy loads, and fatigue damage to these components is inevitable. Further, the methods for predicting the long-term performance of components after reinforcement are not sufficient.

Numerical simulation can examine the creep effect of beams subjected to fatigue damage. On the one hand, the mechanisms for the fatigue damage to typical strengthened concrete beams are studied by fatigue crack propagation theory and cumulative damage theory [18]. Cumulative damage theory studies the fatigue damage accumulation of the material or component and the degree of the fatigue damage, which can be roughly divided into linear cumulative damage theory and nonlinear cumulative damage theory [19–21]. On the other hand, theoretical calculations, such as the differential equation solution method of concrete section stress and steel stress redistribution under shrinkage creep [22] and the effective modulus method adjusted by age [23,24], can simulate the beam creep effect after section reinforcement. So far, no work has combined both fatigue damage and reinforcement to study creep properties.

Considering this background, we develop a numerical model on the basis of continuous damage mechanics to simulate the creep of fatigue-damaged concrete beams. The accuracy of the proposed model is verified by conducting creep tests on fatigue-damaged concrete beams. This work investigates the mechanism for the effect of damage on the creep of concrete members. The novelty of the study is that the numerical model can be employed to analyze the creep of strengthened damaged beams. The analysis can provide scientific guidance for the reinforcement design of fatigue-damaged components.

## 2. Numerical Method

The creep test has drawbacks, such as long experimentation periods, difficult data measurement, and susceptible test results. Numerical simulation studies can analyze the effect of creep on structures in multiple steps and over a long period and obtain time-varying stress–strain data on structures or components. They also play an instructional role in academic studies on the effect of creep on concrete structures. Consequently, this study uses a numerical simulation method to study the creep deformation of fatigue-damaged beams after being strengthened. It uses a subroutine of User Programmable Features (UPFs), i.e., the secondary development tools of ANSYS, called USERMAT, to code the constitutive creep model of damaged concrete. During the operation of ANSYS, the numerical simulation analysis of damaged components can be realized by continuously calling the USERMAT subroutine.

### 2.1. Constitutive Fatigue Model

The damage variable ( $D$ ) is used to define the degree of damage to materials in continuum damage mechanics, and it is shown in Equation (1) [25]. The constitutive

relationship of materials under coupled damage can be achieved through effective stress theory and equivalent strain theory.

$$D = 1 - \frac{\bar{E}}{E} \quad (1)$$

where  $\bar{E}$  can be considered as the elasticity modulus of the damaged material, and  $E$  is the Young's modulus.

- The effective stress theory

The Cauchy stress on the initial cross section of the micro-element of the undamaged material is  $\sigma$ . The stresses on the initial cross section of the micro-element differ between undamaged and damaged materials. The effective stress  $\bar{\sigma}$  on this cross section can be expressed by the Equation (2).

$$\bar{\sigma} = \frac{\sigma}{1 - D} \quad (2)$$

- The equivalent strain theory.

It is assumed that the solid material is an isotropic homogeneous elastomer and that the object is originally in a stress-free natural state. The equivalent strain theory holds that the deformation state of damaged materials under uniaxial or multiaxial stress state can be expressed by the original undamaged material intrinsic law. As shown in Figure 1, the Cauchy stress is replaced by the effective stress in the intrinsic relationship equation.

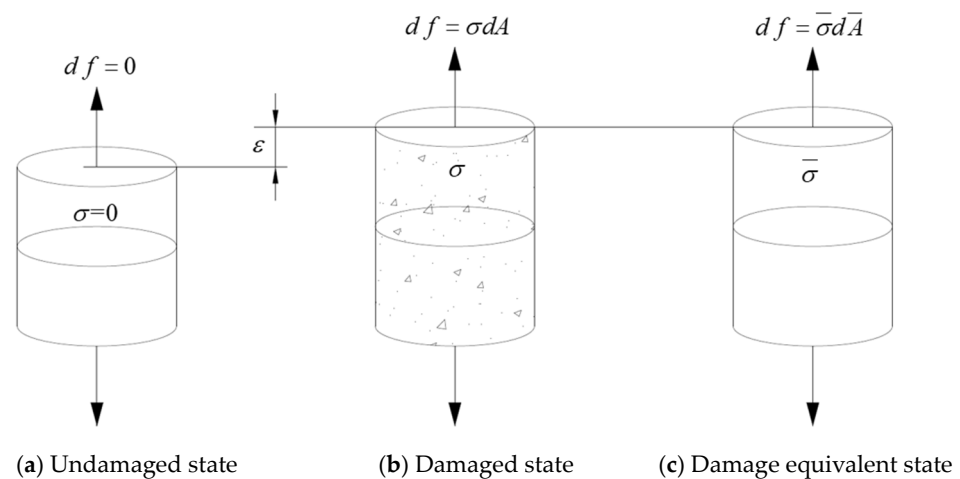


**Figure 1.** The constitutive relationship of materials under damage. ( $df$  represents the force of micro-element,  $dA$  is the area of micro-element,  $\bar{dA}$  is the effective area of micro-element, and  $\varepsilon$  denotes the strain).

When the stress is replaced by effective stress, the constitutive relation of undamaged materials can express the strain of damaged materials [25]. Equation (3) defines the constitutive relation of coupled damage as:

$$\varepsilon_{ij} = \frac{1 + \nu}{E} \frac{\sigma_{ij}}{1 - D} - \frac{\nu}{E} \frac{\sigma_{kk} \delta_{ij}}{1 - D} \quad (3)$$

where  $\sigma_{ij}$  and  $\varepsilon_{ij}$  are the stress and strain tensors, respectively,  $\delta_{ij}$  indicates Kronecker delta,  $\sigma_{kk}$  is volume stress,  $\nu$  represents Poisson's ratio, and  $E$  is the elastic modulus.

The concrete part of the component deteriorates under fatigue loading. This study employs the model for the fatigue damage to concrete based on damage mechanics proposed by Mai et al. [26] to define the damage state and damage distribution after fatigue loading:

$$\dot{D} = \frac{\frac{1}{S(\varepsilon)}}{\frac{m(D)}{1-D} - m'(D) \ln(1-D)} h(f) \left\langle \frac{\partial S(\varepsilon)}{\partial \varepsilon} : \dot{\varepsilon} \right\rangle^+ \varepsilon_{ij} \quad (4)$$

where  $D$  is the damage variable,  $\dot{D}$  denotes the rate of change in the damage variable,  $\varepsilon$  represents the strain tensor,  $m(D)$  indicates the material parameters,  $S(\varepsilon)$  is the damage driving source determined by the strain tensor,  $h(f)$  is a continuous and increasing function such that  $h(0) = 0$  and  $h(1) = 1$ , and  $\langle \cdot \rangle^+$  stands for the positive scalar function, namely  $\langle x \rangle^+ = \frac{1}{2}\{x + |x|\}$ .

Equation (5) defines  $m(D)$  as:

$$m(D) = m_1(1-D)^{m_2} + m_3 \quad (5)$$

where  $m_1$ ,  $m_2$ , and  $m_3$  are the material characteristic parameters determined through experimentation. Section 5.1 presents their specific values.

Equation (6) defines  $h(f)$  as:

$$h(f) = \begin{cases} \alpha^{n_1} \left(\frac{f}{\alpha}\right)^{n_2} & 0 \leq f \leq \alpha \\ f^{n_1} & \alpha < f \leq 1 \end{cases} \quad (6)$$

where  $\alpha$ ,  $n_1$ , and  $n_2$  indicate the material characteristic parameters measured by experimentation. Their specific values are listed in Section 5.1.

Equations (7) and (8) can express  $f$  and  $S(\varepsilon)$ , respectively:

$$f = \frac{(1-D)^{m(D)} S(\varepsilon)}{W} \quad (7)$$

where  $W$  is the initial damage threshold.

$$S(\varepsilon) = \mu \left\{ \left( \langle \varepsilon_1 \rangle^+ \right)^2 + \left( \langle \varepsilon_2 \rangle^+ \right)^2 + \left( \langle \varepsilon_3 \rangle^+ \right)^2 \right\} + \frac{1}{2} \lambda \left( \langle \varepsilon_1 + \varepsilon_2 + \varepsilon_3 \rangle^+ \right)^2 \quad (8)$$

where  $\varepsilon_1$ ,  $\varepsilon_2$ , and  $\varepsilon_3$  are the principal strains,  $\lambda = \frac{\nu E}{(1+\nu)(1-2\nu)}$ , and  $\mu = \frac{E}{2(1+\nu)}$ .

## 2.2. Constitutive Creep Model with Fatigue Damage

The stresses on the initial cross section of the micro-element differ between undamaged and damaged materials. Considering the influence of damage, effective stress  $\bar{\sigma}$  is used to replace the stress on the damaged material on the basis of the assumption of strain equivalence. The effective stress on damaged materials in the solution process is completed in Section 2.1. The principal covariance structure considering the initial damage is applied to the solution process of the numerical simulation.

This study adopts the creep prediction model proposed by Zhu for the numerical simulation of the creep of the concrete beam [27]. Assuming that the stress in each time period is varying linearly:

$$C(t, \tau) = (f_1 + g_1 \tau^{-p_1}) \left[ 1 - e^{-\gamma_1(t-\tau)} \right] + (f_2 + g_2 \tau^{-p_2}) \left[ 1 - e^{-\gamma_2(t-\tau)} \right] \quad (9)$$

where  $C(t, \tau)$  is in the loading period of  $\tau$  and the moment of the creep degree of  $t$ ,  $f_1$ ,  $g_1$ ,  $p_1$ ,  $\gamma_1$ ,  $f_2$ ,  $g_2$ ,  $p_2$ , and  $\gamma_2$  represent the parameters determined by the standard creep test of concrete. Section 5.1 displays the specific values of these tabulated parameters.

### 2.3. Numerical Modeling of Creep Deformation with Fatigue Damage

We develop the constitutive creep model for damaged concrete using the USERMAT subroutine. The consistent tangent operator matrix is calculated for each step of the iterative process on the basis of this constitutive model. The stress increment can be deduced according to the matrix and the strain increment in the last step. Figure 2 illustrates the flow chart for the USERMAT subroutine.

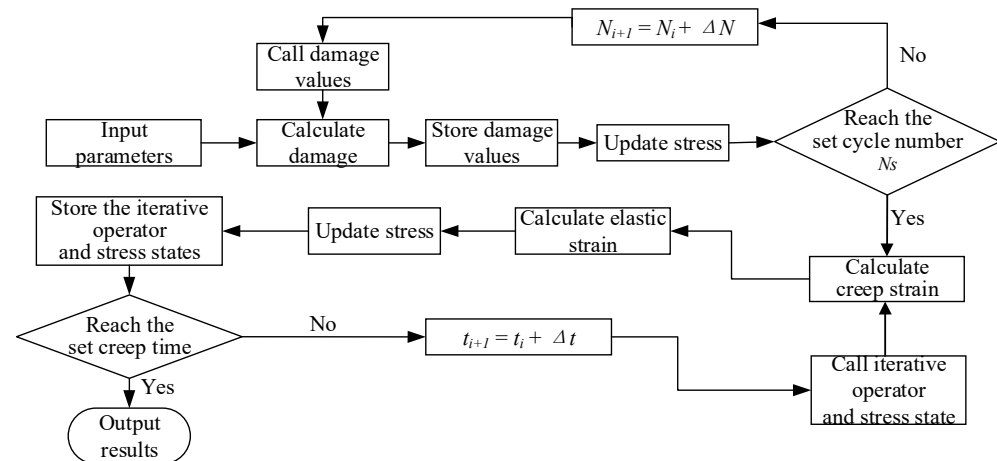


**Figure 2.** The flow chart for subroutine USERMAT:  $N_i$  denotes the number of cycles,  $N_{i+1}$  means the number of cycles after increase,  $\Delta N$  indicates cycle increment,  $t_i$  represents time,  $t_{i+1}$  is the time after increase, and  $\Delta t$  denotes time increment.

Numerical simulation is divided into two main processes: introducing the initial damage and analyzing the creep effect.

#### (a) Introducing initial damage

Introducing fatigue damage is simulated by coding and calling the USERMAT subroutine. The coding consists of two parts:

- Calculating the stress increment using the strain increment ( $\Delta \epsilon$ ) and updating the stress in ANSYS;
- Calculating the Jacobi matrix  $[P] = \frac{\partial \Delta \sigma}{\partial \Delta \epsilon} = [Q]^{-1} \bar{E}$  according to Equations (17) and (20).

The state variable USTATEV in the user material subroutine of ANSYS records and saves the damage variable ( $D$ ) during the operation, which is called and updated in the subsequent operation steps. After coding, the numerical simulation analysis of the damaged materials can be realized by continuously calling USERMAT during the ANSYS runtime.

Essentially, the stress and the damage variable are updated under coupling the stress-strain and damage fields. The specific process is as follows:

- Initialize the material parameters and set the initial value of damage to each element at zero;
- Check whether the time value corresponding to the current cycle number ( $N_i$ ) reaches the preset cycle number ( $N_s$ ), and if not, call the fatigue part of the subroutine;
- Call the equation solver: first, read the accumulated value of the damage variable stored in the previous cycle  $D_i$ , then solve the constitutive relationship depending on Equation (3), and finally, calculate the stress coupled damage under this cyclic loading;
- As a precondition for ensuring the calculation accuracy and saving computing time, this study adopts a jumping algorithm [28]. Take 1% of the fatigue life as the value of cycle increment  $\Delta N$  and solve Equation (4) to calculate the damage increment  $\dot{D}$ ;
- Store the damage variable  $D_{i+1} = D_i + \dot{D} \cdot \Delta N$ , substitute the cumulative value of damage into Equation (3) to solve the constitutive relationship, and update the damaging stress;
- End the iteration if the required number of cycles is reached.

## (b) Creep simulation

The concrete creep model describes the strain growth under constant stress. In the numerical simulation, the time ( $t$ ) is divided into smaller periods, and for each  $\Delta t$ , the corresponding equilibrium equation is established to find the increment of stress in this period. Figure 3 shows this process. Stress history plays a crucial role in creep deformation [29]. Generally, the cumulative creep deformation at a specific time can be realized by calculating and storing the stress values of each element in the finite element model at all times. Zhu [30] proposed an improved explicit algorithm with variable step size and an implicit algorithm.

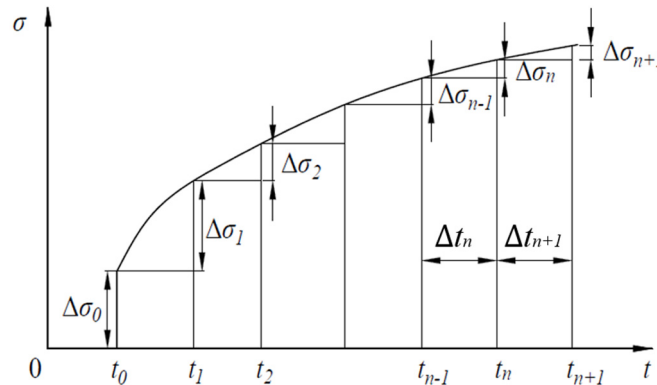


**Figure 3.** The relationship between the stress increment and time used in the calculations of the USERMAT subroutine.

The process is as follows [30]: The creeping time is divided into several periods, namely  $\Delta t_1, \Delta t_2, \dots, \Delta t_n$ , where  $\Delta t_n = t_n - t_{n-1}$ ;  $\Delta \bar{\sigma}_i$  represents the effective stress increment in step  $i$ , and Equation (10) calculates the creep strain at any time.

$$\varepsilon^c(t) = \Delta \bar{\sigma}_0 C(t, t_0) + \int_{t_0}^t C(t, \tau) \frac{d\bar{\sigma}}{d\tau} d\tau \quad (10)$$

If  $\Delta t_n$  is small enough,  $C(t, \tau)$  can be replaced by  $C(t, t_{n-0.5})$  at the midpoint. Thus, Equation (10) can be rewritten as:

$$\varepsilon^c(t_n) = \Delta \bar{\sigma}_0 C(t_n, t_0) + \sum_{i=1}^n \Delta \bar{\sigma}_i C(t_n, t_{i-0.5}) \quad (11)$$

The creep strain increment is also given by:

$$\Delta \varepsilon_n^c = \Delta \bar{\sigma}_0 [C(t_n, t_0) - C(t_{n-1}, t_0)] + \sum_{i=1}^{n-1} \Delta \bar{\sigma}_i [C(t_n, t_{i-0.5}) - C(t_{n-1}, t_{i-0.5})] + \Delta \bar{\sigma}_n C(t_n, t_{n-0.5}) \quad (12)$$

Equation (9) can be rewritten as:

$$C(t, \tau) = \sum_{i=1}^2 \varphi_i(\tau) [1 - e^{-\gamma_i(t-\tau)}] \quad (13)$$

where  $\varphi_i(\tau) = (f_i + g_i \tau^{-p_i})$ .

Equation (12) can be written as:

$$\Delta \varepsilon_n^c = \sum_{i=1}^2 (1 - e^{-\gamma_i \Delta t_n}) \omega_{i,n} + \Delta \bar{\sigma}_n C(t_n, t_{n-0.5}) \quad (14)$$

where  $\omega_{i,n} = \Delta\bar{\sigma}_0\varphi_i(t_0)e^{-\gamma_i(t_{n-1}-t_0)} + \sum_{m=1}^{n-1} \Delta\bar{\sigma}_m\varphi_i(t_{m-0.5})e^{-\gamma_i(t_{n-1}-t_{m-0.5})}$ , and the recursive formula for the iterative operator can be defined as:

$$\omega_{i,n} = \omega_{i,n-1}e^{-\gamma_i\Delta t_{n-1}} + \Delta\bar{\sigma}_{n-1}\varphi_i(t_{n-1-0.5})e^{-0.5\gamma_i\Delta t_{n-1}} \quad (15)$$

where  $\omega_{i,1} = \Delta\bar{\sigma}_0\varphi_i(t_0)$ , and  $\omega_{i,n}$  is the iterative operator.

The creep of the concrete structure can be analyzed by storing  $\omega_{i,n}$  without recording the stress history, which remarkably saves the storage. For the material constitutive model defined by the user subroutine, it is necessary to calculate the stress increment ( $\Delta\bar{\sigma}_n$ ) through the strain increment ( $\Delta\varepsilon_n$ ) imported by the main program. Without considering the temperature strain, Equation (16) expresses the relationship between the stress increment and the strain increment:

$$\Delta\bar{\sigma}_n = [Q]^{-1}E\Delta\varepsilon_n^e \quad (16)$$

where  $E$  is the elastic modulus at the midpoint age, and  $\Delta\varepsilon_n^e$  indicates the increment of the elastic strain.  $[Q]$  and  $\Delta\varepsilon_n^e$  are expressed by Equations (17) and (18), respectively:

$$[Q] = \begin{bmatrix} 1 & -\nu & -\nu & 0 & 0 & 0 \\ -\nu & 1 & -\nu & 0 & 0 & 0 \\ -\nu & -\nu & 1 & 0 & 0 & 0 \\ 0 & 0 & 0 & 2(1+\nu) & 0 & 0 \\ 0 & 0 & 0 & 0 & 2(1+\nu) & 0 \\ 0 & 0 & 0 & 0 & 0 & 2(1+\nu) \end{bmatrix} \quad (17)$$

where  $\Delta\varepsilon_n^e$  indicates the increment of the elastic strain:

$$\Delta\varepsilon_n^e = \Delta\varepsilon_n - \Delta\varepsilon_n^c = \Delta\varepsilon_n - \eta_n - \Delta\bar{\sigma}_n C(t_n, t_{n-0.5}) \quad (18)$$

where  $\eta_n = \sum_{i=1}^2 (1 - e^{-\gamma_i\Delta t_n})\omega_{i,n}$ .

Combining Equation (16) with Equation (18) yields:

$$\Delta\bar{\sigma}_n = [P](\Delta\varepsilon_n - \eta_n) \quad (19)$$

where  $[P] = [Q]^{-1}\bar{E}$ , and  $[P]$  is the consistent tangent operator matrix.  $\bar{E}$  is expressed by Equation (20).

$$\bar{E} = \frac{E}{1 + EC(t_n, t_{n-0.5})} \quad (20)$$

### 3. Modeling

#### 3.1. Simulation Program

In order to study the creep effect of fatigue-damaged concrete structures after being strengthened, we performed numerical simulations under five different working conditions classified in Table 1.

**Table 1.** The working conditions for the numerical simulation of beams.

Numerical Simulation Component Number	Fatigue Cycle (% $N_{max}$ )	Height of Post-Cast Layer (mm)	Loading Age (d)	Load (kN)
F	0%, 2%, 10%, 60%	0, 100	80	10
ST	0%	0	365	5, 10, 15
A	0%, 60%	100	365, 1000, 3650	10
H	0%, 60%	0, 50, 100, 150	365	10
MS	0%, 60%	0, 100	365	10

Note: F: fatigue damage components; ST: sustained loading components; A: components with different loading ages; H: components with different post-cast layer heights; MS: components subjected to a bending moment. For example, F-10%-100-80-10 represents the beam with 10% fatigue damage (the height of the post-cast layer is 100mm) loaded with a load of 10kN for 80 days.

### 3.2. Geometric Models

Figure 4 illustrates the cross-sectional dimensions and reinforcement of the components.

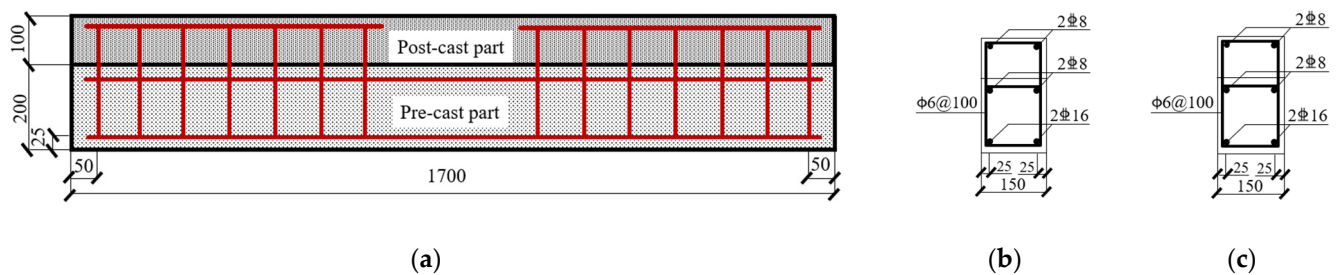


**Figure 4.** The sections and reinforcement of the concrete beams (unit: mm): (a) The cross-sectional dimensions; (b) the positive bending moment section; and (c) the negative bending moment section.

The beam has a rectangular section with a length of 1700 mm and a width of 150 mm; its height depends on the height of the post-cast section, and the concrete cover is 25 mm. The precast section is the existing concrete with dimensions 150 mm × 200 mm. The width of the post-cast part is 150 mm, and its height is set according to the purpose of the study: 0, 50, 100, or 150 mm. The stirrup size of the post-cast part is consistent with that of the precast. Two HRB400 steel bars with a diameter of 8 mm are arranged at the upper part of the section, and two HRB400 steel bars with a diameter of 16 mm are arranged at the lower part of the section under a positive bending moment.

### 3.3. Model Development

Elements solid186 and link180 simulate the concrete and the steel bar, respectively. The reinforcement design in this study ensures sufficient anchorage length, so the reinforcements are firmly anchored in concrete to avoid slippage. Therefore, neither the slippage between new and old concretes nor the slippage between reinforcement and concrete is considered in the modeling process. A fixed hinge support is set at one end of the finite element model, and a rolling hinge support is set at the other. A steel block with high stiffness is set at the support to prevent rapid damage development due to the stress concentration at the support.

Further, there is no slippage between the precast beam and the steel block. The beam adopts the mapping grid, and the grid width of the beam and the steel bar is 25 mm. The precast concrete consists of 3264 elements, and the post-cast concrete comprises 1632 elements; the longitudinal bar consists of 64 elements. Figure 5 displays the finite element model of the composite beam.

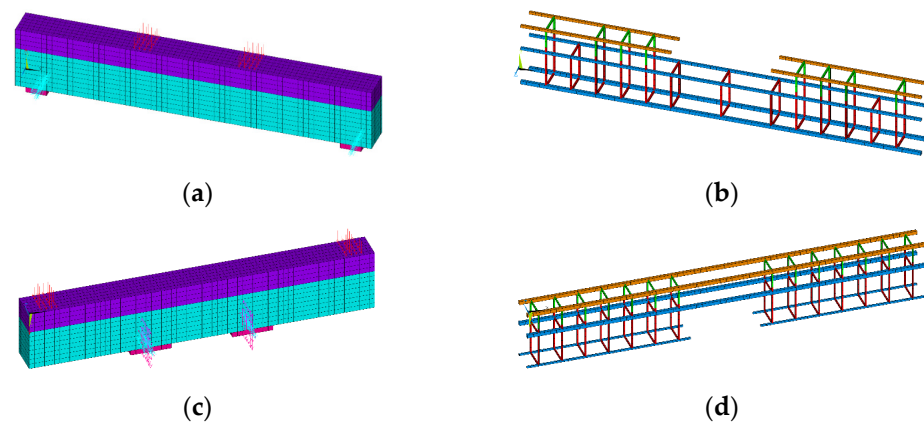


**Figure 5.** The finite element model of the concrete beam: (a) The component under a positive bending moment; (b) the reinforcement skeleton under a positive bending moment; (c) the component under a negative bending moment; and (d) the reinforcement skeleton under a negative bending moment.

In this study, both the reinforcement and the concrete are under low stress during the loading process due to the slight creep loading. Under such circumstances, the creep of concrete components is affected more by the concrete and less by the reinforcements. Therefore, a bilinear isotropic strengthening model is adopted for the steel bars. The numerical simulation process is divided into two stages, namely fatigue damage introduction and creep loading, realized by two loading steps. The superposition of the post-cast concrete is realized by the life-and-death element method in ANSYS software. The element corresponding to the superimposed layer is activated after the fatigue loading step but before the creep loading step, and its damage variable is set to zero.

#### 4. Experimental Procedures

Static loading test, fatigue loading test, and creep experiment were conducted to validate the accuracy and applicability of the numerical model proposed herein. The deflection and strain of the specimens were measured and recorded during testing.

##### 4.1. Materials

PO 42.5 Portland cement was used as the binder, and the coarse aggregate was crushed stones with a continuous gradation of 5–16 mm; the fine aggregate was river sand. Further, a similar mix proportion presented in Table 2 was used for the precast beam and the lamination layer of concrete. The designed compressive strength of concrete was 30.0 MPa, and the measured 28-day compressive strength of cubic concrete specimens was 30.9 MPa. The measured elastic modulus of the concrete was also 22.9 GPa.

**Table 2.** The mix composition of the concrete.

Ingredient	Water	Cement	Fine Aggregate	Coarse Aggregate
Value (kg/m <sup>3</sup> )	210	382	651	1157

The specifications and types of the reinforcement are as described in the numerical simulation model, and Table 3 lists the main mechanical properties of the steel bars.

**Table 3.** The main mechanical properties of the steel bars.

Type	Yield Strength (MPa)	Ultimate Strength (MPa)	Young's Modulus (GPa)
HPB300	300	446	206
HRB400	465	612	195

#### 4.2. Section Design

The cross-sectional design is consistent with the numerical model. According to code GB50010-2010 [31], the stirrups of the precast beam should be extended into the lamination layer to guarantee the overall stability of the composite concrete beam. The internal hoops of the cast-in-place concrete are not closed hoops after this setting. On the other hand, cracks generated by fatigue damage are randomly distributed in the concrete [32]. Although the beam undergoes bending failure under static loading, the oblique section shear failure may occur under fatigue loading [33]. Therefore, the shear capacity of the precast beams is guaranteed by adhering carbon fibers to the inclined section to ensure that they do not undergo shear failure during fatigue loading [34–36]. The reinforcement schematic is shown in Figure 6.

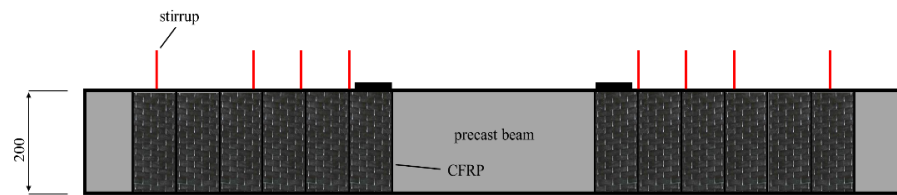


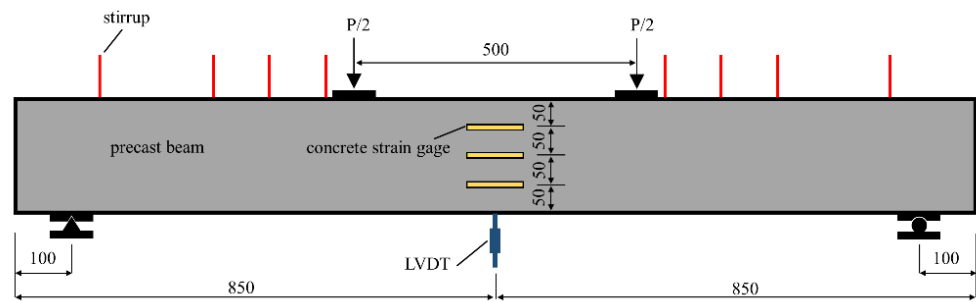
**Figure 6.** A schematic of the carbon fiber reinforcement method (unit: mm).

The design of carbon fiber reinforcement is according to code GB50367-2013 [37]. Carbon-fiber-reinforced plastic (CFRP) is pasted on the shear span of the precast beam, so it has a slight influence on the bending bearing capacity of the beam, which can ensure that the damage to concrete primarily concentrates in the pure bending section in the fatigue test [38]. The CFRP is U-shaped, is pasted on the whole side and bottom of the beam, and has a thickness of 0.111 mm [39]. The design value of the tensile strength of the CFRP is also 1120 N/mm<sup>2</sup>. The CFRP is removed at the end of the fatigue test, and the lamination layer is cast. The purpose of pasting the lamination layer is to improve the load-bearing capacity of the section and prevent the shear failure of the beam. The casting size is shown in Figure 4, and the materials are consistent with the precast part.

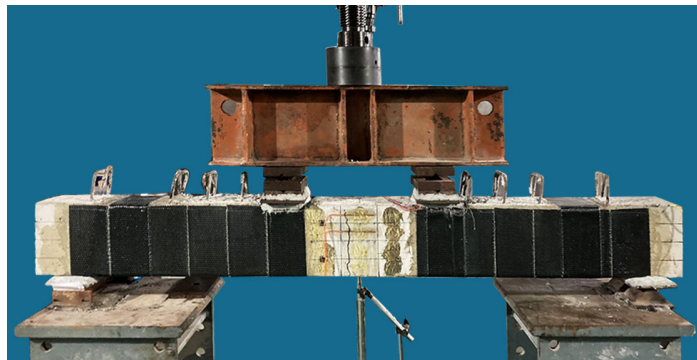
#### 4.3. Introducing Fatigue Damage

Firstly, the static loading test was conducted to measure the ultimate bearing capacity of the beam so as to determine the fatigue load and the creep load. The static loading test was performed in three phases. In the first phase, each stage was loaded with 3.0 kN before cracking, and in the second phase, each stage was loaded with 5.0 kN from cracking to the theoretical ultimate load-bearing capacity of the component (72.6 kN). In the third phase, 3.0 kN was loaded until the component failed. The maximum value under the stable state during loading, i.e., 106.0 kN, was taken as the actual ultimate load-bearing capacity of the component.

According to the test results of static loading, the upper load limit for the fatigue loading was considered 65% of the ultimate bearing capacity of the beam, i.e., 68.9 kN, and the stress ratio was taken as 0.1. Fatigue tests were performed on a PMW800 electro-hydraulic pulsation fatigue loading machine with a loading frequency of 4 Hz. During the fatigue loading, linear variable displacement transducers (LVDTs) were employed to measure the midspan deflection of the beams, and strain gauges were used to record the midspan strain of the beams. A DH5922 dynamic data acquisition instrument synchronously collected the deflection and the strain with a sampling frequency of 100 Hz. Figure 7 illustrates the fatigue loading test on the precast beams.



(a)



(b)

**Figure 7.** The fatigue loading of the precast beams: (a) a schematic of the fatigue loading test (units: mm) and (b) the layout of the fatigue loading test.

The fatigue life of the component was 152,355 cycles, and the failure mode was bending failure. Figure 8 plots the evolution curve of the midspan deflection of the beams during the fatigue test.

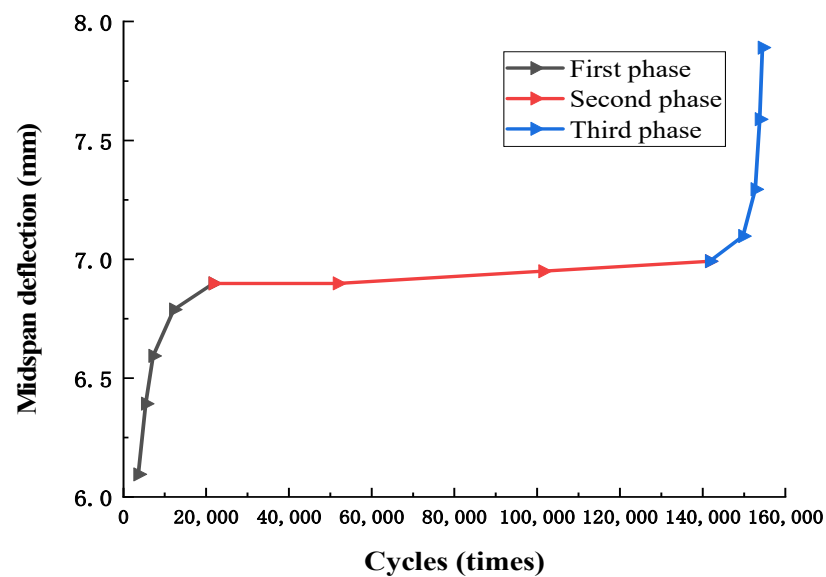


**Figure 8.** The midspan deflection of the beam with a fatigue life of 152,355 cycles.

Figure 8 demonstrates that the midspan deflection of the beam during fatigue loading presents three-phase characteristics. The first phase is the rapid growth of the beam deflection, which accounts for approximately 6.5% of the fatigue life. After that is the stable

fatigue evolution phase, in which the beam deflection develops slowly, accounting for 92.5% of the fatigue life. The last phase is the failure stage, where the midspan deflection of the beam develops rapidly into a brittle fracture. Because the fatigue life of the strengthened concrete beams is discrete, and the third phase of fatigue is rapid and difficult to control, three representative working conditions, namely the first phase of the fatigue, the early stage of the second phase, and the middle and late stages of the second phase, are selected as the three initial damage states. Therefore, the loading cycles for fatigue damage degree of 2%, 10%, and 60% are 3000, 15,000, and 90,000, respectively.

#### 4.4. Creep Experiments

##### 4.4.1. Creep Test on Concrete Specimens

The creep coefficient is an essential material parameter for examining the long-term performance of structures. Different stress levels change only the initial strain of concrete, and the creep development has the same pattern, presenting a similar creep coefficient in the linear creep stage of concrete. Standard creep tests were carried out on two specimens, numbered C1 and C2, to obtain the creep coefficient of the material. Moreover, the standard shrinkage test was conducted on specimen SK to assess the shrinkage strain of the concrete. All the above tests were performed at a temperature of  $20 \pm 2$  °C and a relative humidity of  $60 \pm 5$ %.

The specimen was loaded by a spring-type creep meter, and the data were recorded by a micrometer and displayed in real time by a pressure sensor. Figure 9 displays the layout of the experiments.

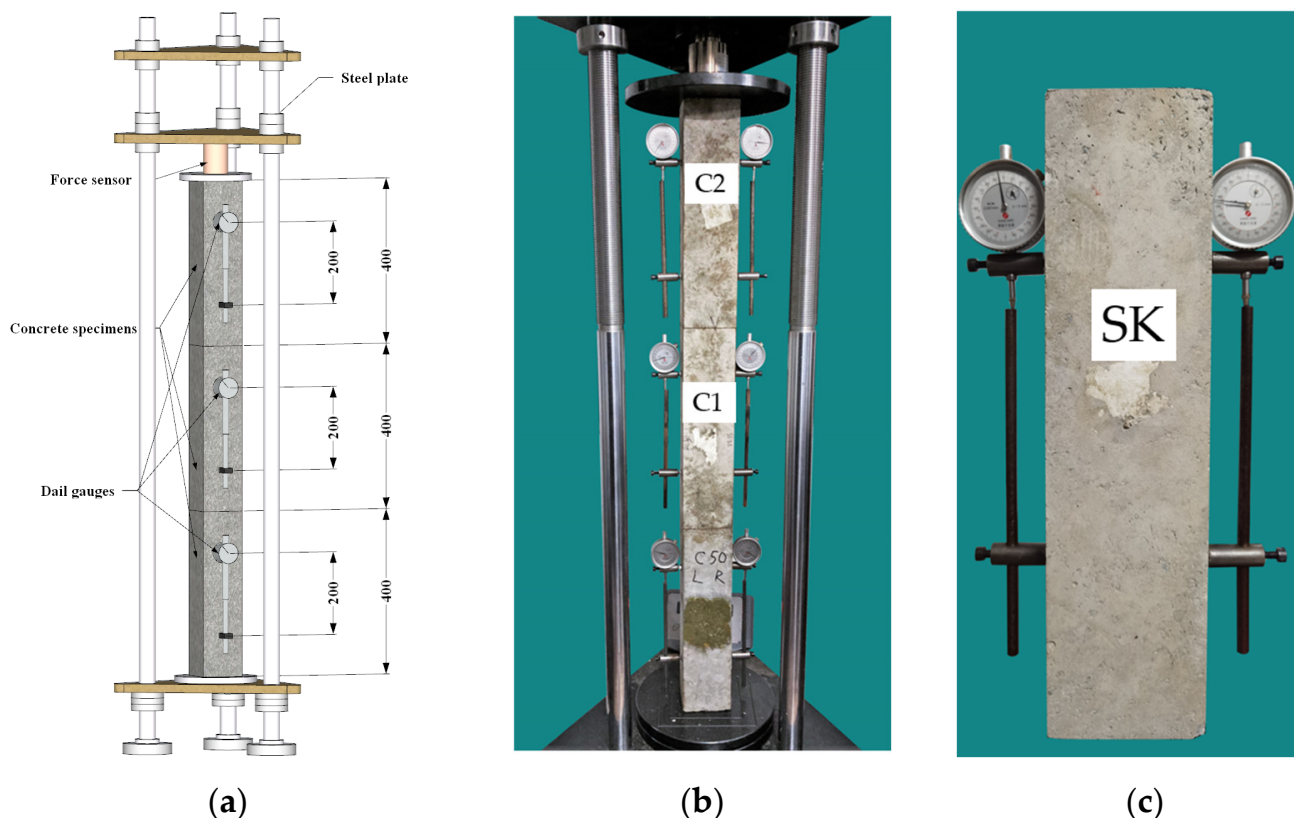


**Figure 9.** The creep and shrinkage experiments on the concrete specimens: (a) a schematic of the creep loading test, (b) the creep loading test and (c) the shrinkage test. (C1 and C2 are standard creep tests specimens, SK is shrinkage test specimen).

As shown in Figure 9, a jack applied a creep load equal to 30% of the ultimate load, and the pressure was maintained at a changeless level by an adjustable spring. The deformation of the concrete specimen was recorded by dial gauges installed on the opposite surface of



creep test results of C1 and C2. Table 5 shows the tabulated fitted parameters of the creep model.

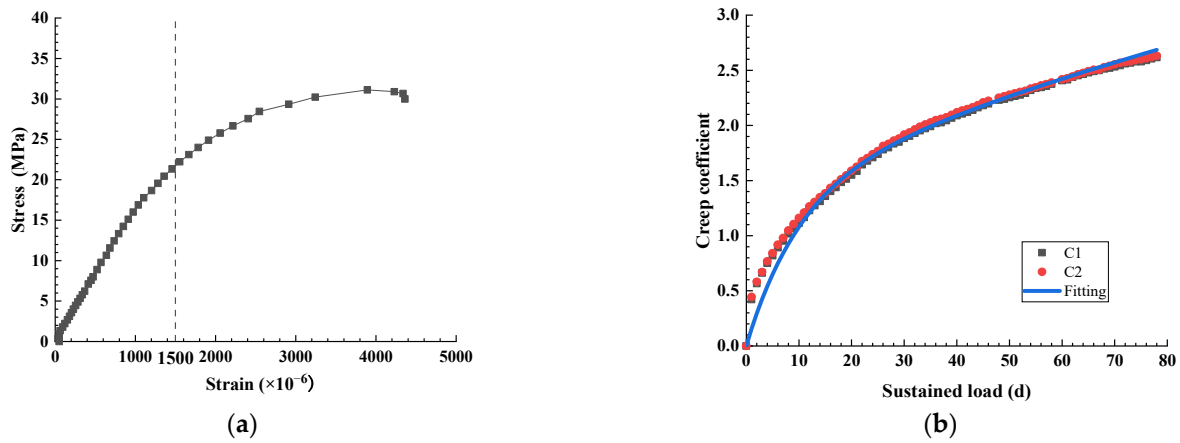


Figure 11. The properties of concrete: (a) uniaxial stress–strain and (b) the creep curves of the concrete.

Table 5. The fitted parameters of the creep model.

Parameter	$f_1$	$g_1$	$p_1$	$\gamma_1$	$f_2$	$g_2$	$p_2$	$\gamma_2$
Value	$1.94/E$	$17.848/E$	0.45	0.003	$0.67/E$	$1.139/E$	0.45	0.1

### 5.2. Comparing Experimental Results with Numerical Data

#### 5.2.1. Midspan Deflection

Figure 12 delineates the numerical and experimental midspan deflection and midspan deflection increment of the components.

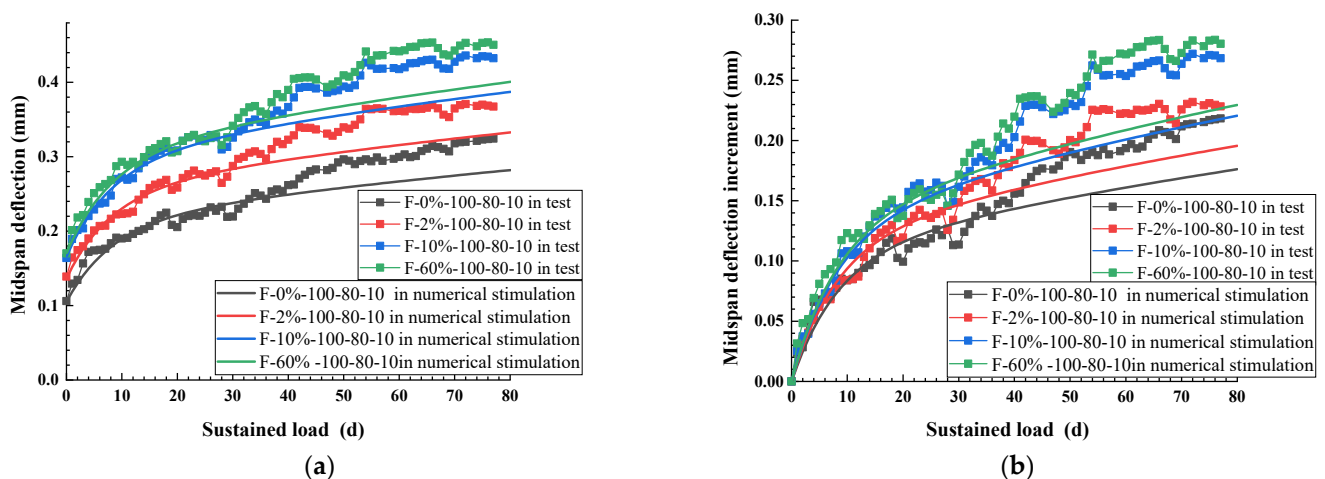


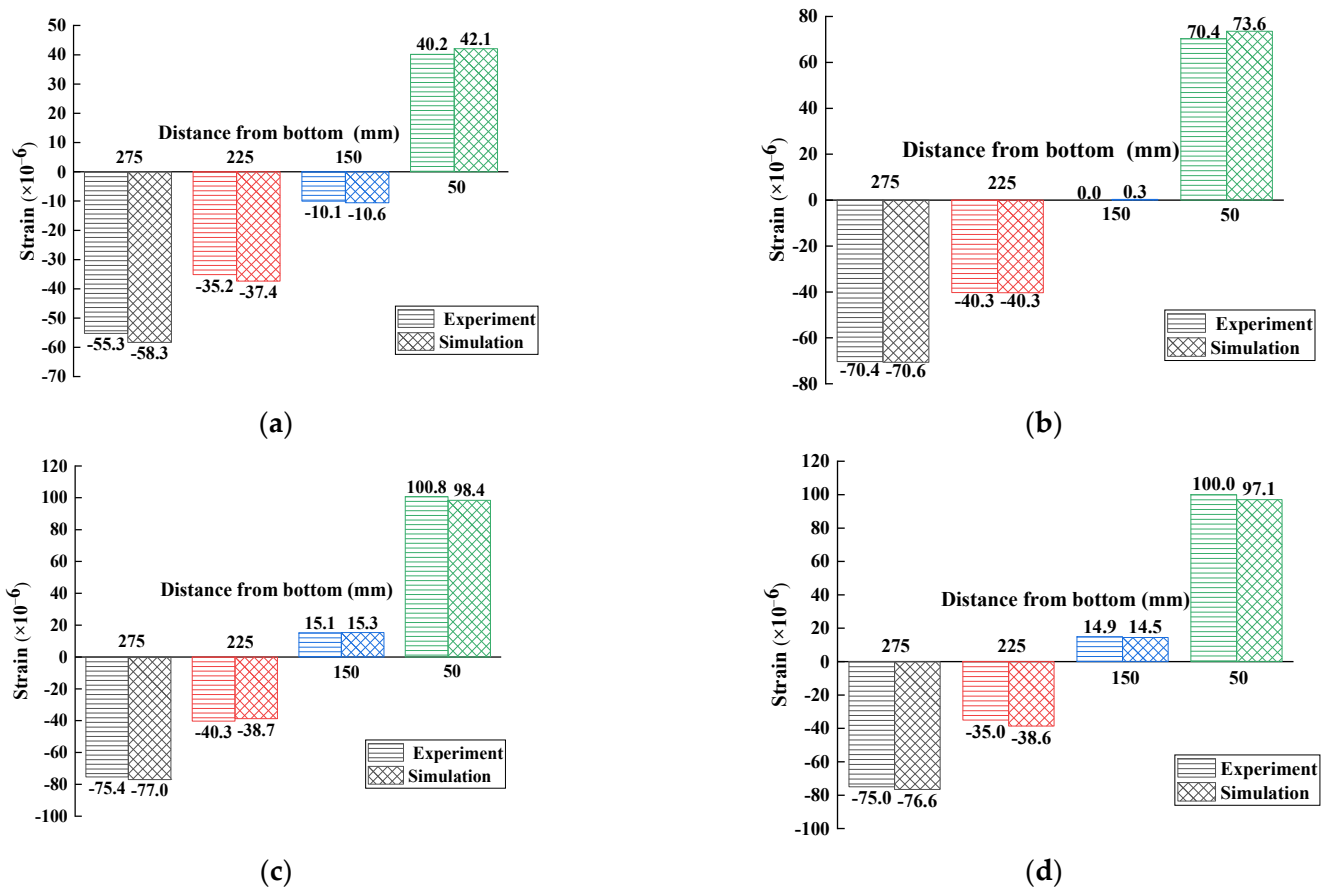
Figure 12. The evolution of the (a) midspan deflection and (b) midspan deflection increment during fatigue loading.

According to Figure 12, the higher the degree of damage to the precast beam, the more significant the midspan deflection and midspan deflection increment of the composite beam in the initial creep stage. The deflection increment is more suitable for characterizing the creep deflection of the strengthened damaged concrete beams. Comparing the experimental results of each component with the numerical data reveals that both are close in the first 40 days of loading; the experimental values are slightly higher than the numerical ones in the later stages, but the difference in the numerical and experimental deflections is less

than 15%. The test results fluctuate to a certain extent due to the influence of environmental temperature and humidity on concrete creep. Therefore, the numerical simulation method used to explore the influence of fatigue damage on the creep of the beams, i.e., their midspan deflection, is practical.

### 5.2.2. Stress on Cross Section

As the concrete was being loaded, its strain was evaluated at a distance of 50, 150, 225, and 275 mm from the bottom of the beam. The concrete strain was measured along the height of the concrete section by pasting dial gauges on its surface. According to the tests by Tang [41] and Fang [13], the strain variation caused by the concrete shrinkage of the old and new concrete of composite components is significant, and it is challenging to completely distinguish the creep strain from the shrinkage strain in tests. Therefore, this study compares only the experimental elastic strain in the midspan section of the composite beams with the simulated data, as shown in Figure 13.



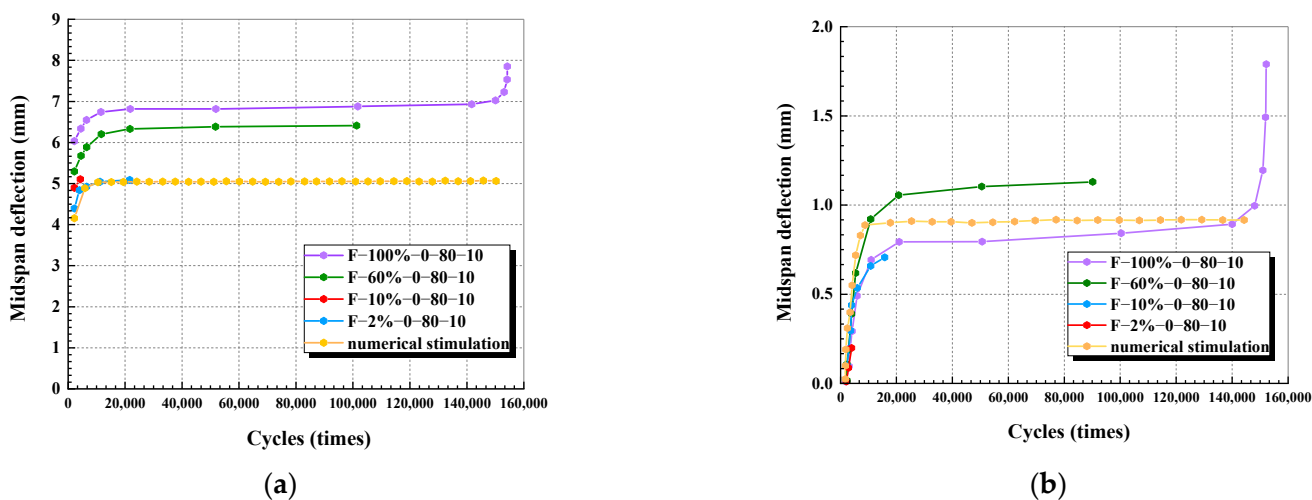
**Figure 13.** Comparing the elastic strain in the midspan section of the composite beams: (a) F-0%-100-80-10; (b) F-2%-100-80-10; (c) F-10%-100-80-10; and (d) F-60%-100-80-10.

Figure 13 shows that the numerical elastic strains calculated without considering the shrinkage effect are closer to the experimental results. The simulation of the creep effect for the fatigue-damaged components is closer to the actual situation, verifying that the developed numerical method is practical.

### 5.3. Fatigue damage

There is a difference in the shrinkage strains between the precast and post-cast parts of the composite beams, leading to additional deflection. This study employs the calculation method of additional deflection proposed by Zhu to correct the deflection [28,29]. Figure 14a delineates the variation in the numerical and experimental maximum midspan

deflection of the beams with the fatigue cycles. Figure 14b plots the change in the numerical and experimental maximum midspan deflection increment of the beams with the fatigue cycles. Figure 14 demonstrates that the development of the deflection of each precast beam follows similar trends in the fatigue tests and the numerical simulation. The numerical and experimental trends of the maximum midspan deflection increment of the beams are also close.



**Figure 14.** The development of the (a) midspan deflection and (b) midspan deflection increment during fatigue loading.

## 6. Discussion

Many factors affect the shrinkage and creep performance of materials, such as composition [42], temperature, and humidity [43]. The stress on beams and the concrete age at loading are the main factors affecting the creep deformation, but the influence of these factors is not evident. Therefore, it is necessary to discuss the mechanism for the effect of damage on the creep development of beams. Although increasing the section is a standard method for structural reinforcement [44], it is still worth examining the creep of damaged components after being strengthened.

### 6.1. Factors Influencing Damage Effect on Creep of Strengthened Beams

#### 6.1.1. Stress Magnitude

The essential impact of damage on the creep of concrete beams is the degradation of the cross-sectional stiffness, which leads to the difference in the stress distribution of the cross section under the same load. The creep effect depends on the stress state of the beams, so a difference in the cross-sectional stress distribution causes a difference in the creep effect. Hence, this section presents the investigation of the mechanism for the effect of damage on the creep development of the beams through experiments with different sustained loads applied to the undamaged components. The components are described in Section 3.1, and Figure 15 depicts the test results.

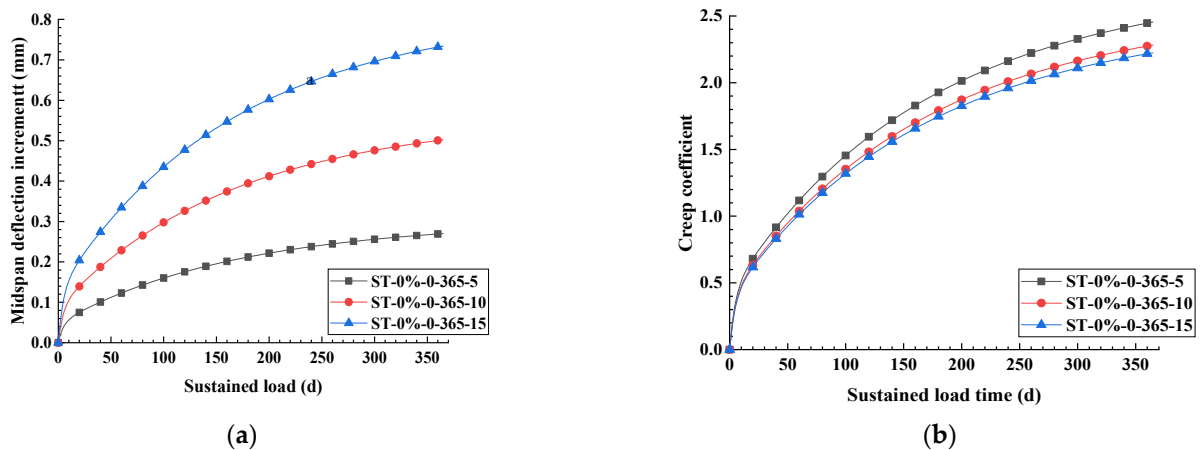


**Figure 15.** The (a) midspan deflection increment and (b) creep coefficient of the concrete beams under different stresses.

Figure 15a shows that the midspan deflection increment of the concrete beams is significantly higher under larger loads because creep correlates closely with the distribution and magnitude of stress on concrete. The undamaged beams are continuously loaded with 5 and 15 kN for 365 days, with midspan deflections of 0.270 and 0.734 mm, respectively. Although the distribution of stress on the beam is not uniform, the stress on the beams under large loads is generally higher than that on the beams under small loads. This is also why the strain of the beams under large loads is generally higher than that of the beams under small loads.

According to a previous study, the creep of concrete components is proportional to the stress when the stress on them is lower than 40% of their strength [45]. The creep coefficient is similar to this case. It can be inferred from Figure 15a that there is a distinct difference in the creep coefficients of the three components: the creep coefficients of the beams under larger loads are relatively smaller. This is because the stresses at various points of the beam constantly change over time and are affected by multiple factors other than the strain effects (see Figure 16). Although the strain is linearly related to the stress under creep, the change in stress does not correlate linearly with the load. As a result, the creep coefficients of the beams under various loads are not identical.

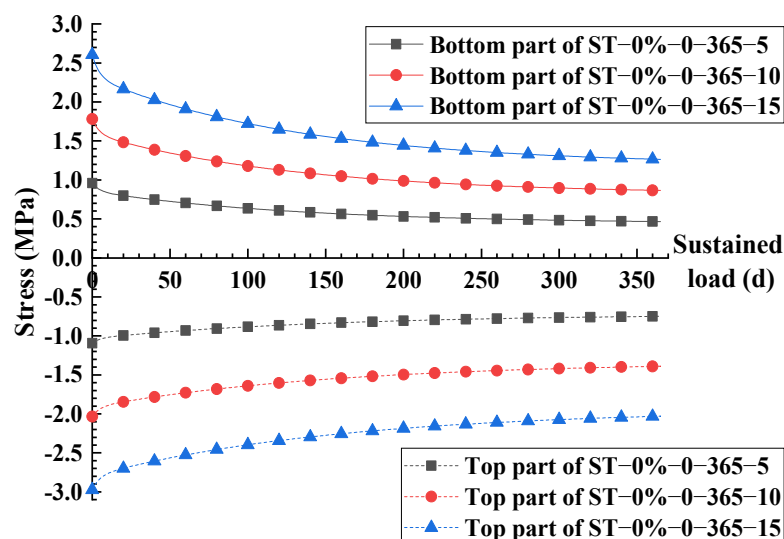


**Figure 16.** Comparing the stress on the beams under creep at various loading levels.

The damage causes the redistribution of the stresses on the concrete in the beam cross section. The initial elastic strain and subsequent strains of the fatigue-damaged beams

increase to some extent because some part of the concrete withdraws from bearing the load (or the effective area is reduced due to the damage), and the remaining concrete is subjected to increased stress under the same bending moment. This leads to the higher deflection of the damaged beam compared with undamaged beams under creep. It should be emphasized that damage gives rise to different stress states and various rates of stress change. Therefore, it is not reasonable to use undamaged components to anticipate the creep strains of damaged components.

### 6.1.2. Loading Age

The age of concrete at loading affects its creep properties, and all creep models consider the loading age a crucial parameter. In order to explore the mechanism for the impact of damage on the creep development of concrete beams, here we apply a sustained load to the fatigue-damaged beams of different ages using the component identities presented in Section 3.1. Figure 17 depicts the change in the deflection increment of and the stress on the fatigue-damaged concrete beams of different ages with the loading time.

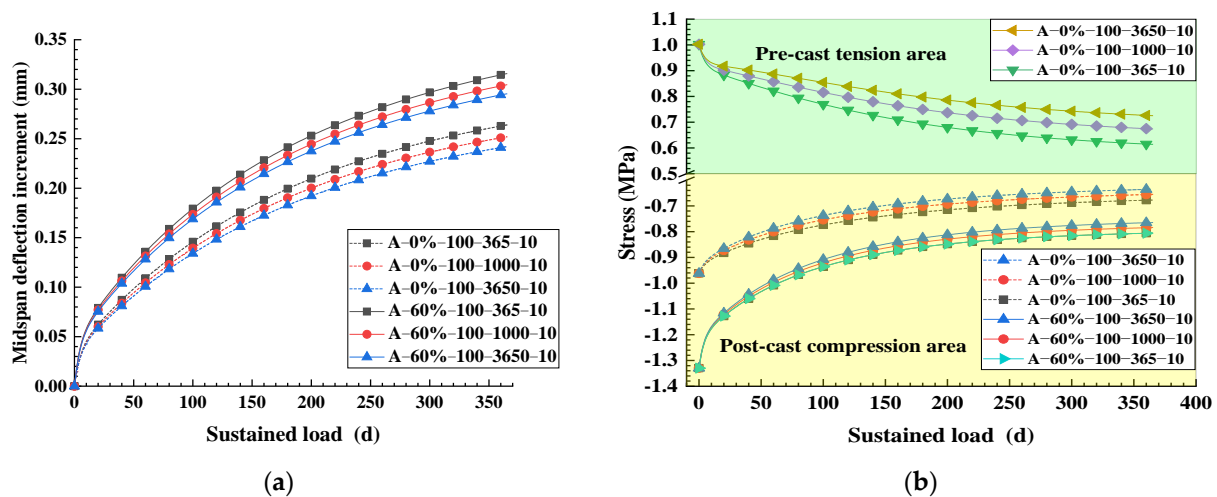


**Figure 17.** The creep effect of the fatigue-damaged concrete beams of different ages under loading: (a) the midspan deflection increment and (b) the section stress.

According to Figure 17a, if the additional deflection caused by the difference in the beam shrinkage is not taken into account, the deflection of both damaged and undamaged laminated components under the influence of creep diminishes with age. The deflection of beam A-60%-100-365-10 and beam A-60%-100-3650-10 is 0.252 mm and 0.264 mm at the age of 365 and 3650 days, respectively. It increases by approximately 0.01 mm in 3285 days. For the same material, creep declines with increasing the loading age. This law is also reflected in the creep model used in this paper. A lower creep results in a lower creep strain for the same stress state, leading to a smaller beam deflection. For the same loading age, damage to the beams enlarges their midspan deflection increment, implying that raising stress increases the creep of the beams.

Figure 17b demonstrates that the stress on the top of the beam in the post-cast part is lower for the damaged and undamaged beams with longer ages. After 3650 days, the stress on the precast concrete of the undamaged beam is 0.7 MPa, while that on the post-cast concrete is  $-0.7$  MPa. The stress on the old concrete is approximately 1.4 MPa greater than that on the new concrete. However, for the precast section, the tensile stress on the beam with a longer age is higher and varies slightly with time. Indeed, the components with a more extended age have lower creep strains, and the smaller strain reduces the change in stress.

Under similar initial stress, the stress on the components with a longer age is always more considerable under the effect of creep. In contrast, at a similar loading age and creep,

the difference in the strain of the midspan section of the beams directly causes the difference in the stress on them. The strain of the components with a more extended age is lower in the span of the precast part, which is the opposite of the previously mentioned stress variation law. Since the stress on the precast part of damaged beams is coupled with the effect of damage, it is impossible to directly and accurately determine the stress, but the law of undamaged beams can deduce it: the stress increases with the loading age under the creep effect. Nonetheless, the deflection of the beams is relatively small, so the loading age can affect the creep of damaged components and the stress state.

As mentioned above, the loading age is one factor affecting the creep development due to damage to concrete beams. The primary mechanism is that increasing the loading age reduces the degree of creep and the creep coefficient at the same loading time and declines the creep strain in the same stress state, which not only gives rise to the difference in the development of the deflection of the beams under creep but also leads to the difference in the stress state after loading. The effect of creep also depends on the loading age or its creep properties. Although the loading age can be controlled in experimentation or numerical simulation, in practical engineering, the damage is often accompanied by a long loading age, and even the degree of damage is coupled with the loading age. Therefore, the impact of the loading age cannot be neglected in the creep analysis.

## 6.2. Creep Effect of Strengthened Damaged Beams

The discussion in Section 6.1 demonstrates that both the magnitude of the sustained load and the age of the concrete impact the stresses on the strengthened beam section and eventually change the creep effect of the concrete. In fact, when reinforcing the beams by increasing their cross section, the height of the reinforcement significantly impacts the stress state of the component [46] because the height of the reinforcement affects the creep effect of the component. Thus, this section discusses the creep of the damaged beams that were strengthened and subjected to positive and negative bending moments.

### 6.2.1. Under Positive Bending Moment

This section investigates the effect of reinforcing damaged beams on their creep development from a stress perspective. Thus, different heights of the post-cast layer are set for comparison, as described in Section 3.1. Figure 18 presents the test results.

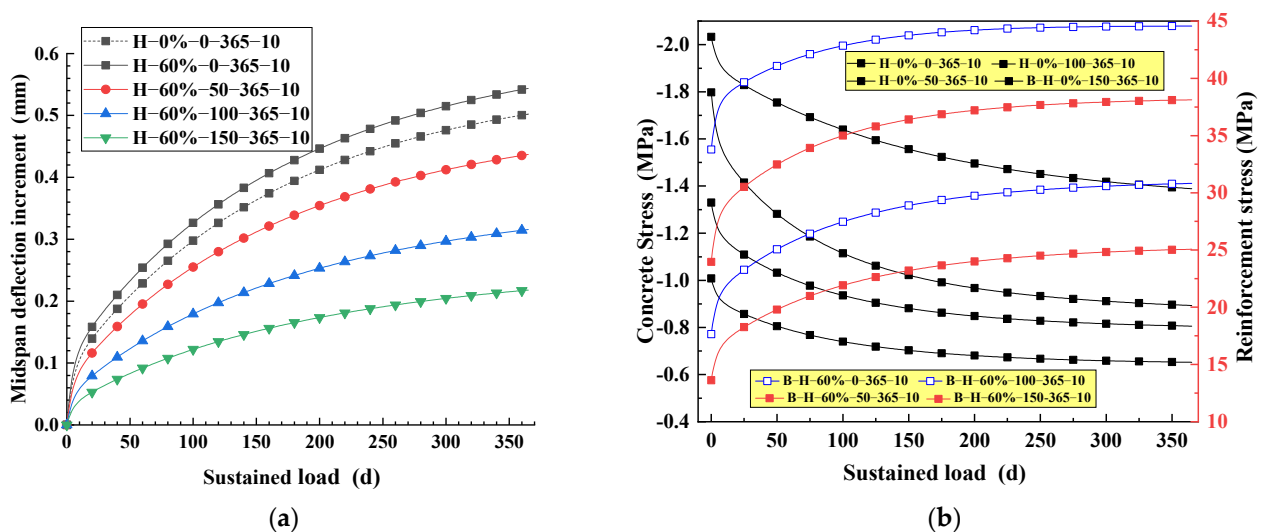


**Figure 18.** The creep of the concrete with different heights of reinforcement under a positive bending moment: (a) the midspan deflection increment and (b) the section stress.

As shown in Figure 18a, the deflection of damaged unstrengthened beam H-60%-0-365-10 increases under the effect of creep compared with undamaged beam H-0%-0-365-10

at a loading period of 365 days. The incremental creep deflection of the beams declines with increasing the height of their reinforcement. The incremental creep deflection of the beams with a strengthened section height of 50, 100, and 150 mm decreases by 0.107, 0.228, and 0.326 mm, respectively, compared with beam H-60%-0-365-10 at a loading period of 365 days. Indeed, increasing the section height makes the damaged components more rigid and weakens the stress state of the section under the same bending moment. Further, the creep strain is slight when the stress is low, reducing the deflection increment of the beams. In addition, the incremental deflection of the strengthened damaged beams is lower than that of the undamaged beams (H-0%-0-365-10). The method of reinforcing damaged beams with laminating post-cast parts promising results in terms of controlling their creep deflection; in particular, increasing the section height has a profound effect.

According to Figure 18b, since the stress on the top of the unstrengthened concrete beams coupled with the effect of damage cannot be depicted realistically, the stress on the damaged beams under the effect of creep should be higher than that on the undamaged beam. This figure demonstrates that the stress on the top of the damaged beams declines to some extent during creep after post-cast concrete reinforcement and is lower than that on the undamaged beam (H-0%-0-365-10). Therefore, the reinforcement method of laminating a post-cast concrete part to the damaged beam performs well. The tensile stress on the bottom longitudinal reinforcement of the damaged beams decreases when the height of the reinforcement section increases. However, if the height of the reinforcing post-cast layer reaches 150 mm, the tensile stress on the longitudinal bars of the damaged concrete beams under the effect of creep is similar to that on the undamaged concrete beam (H-0%-0-365-10). Nonetheless, the longitudinal tensile stress on the damaged beam when the height of the reinforcement reaches 150 mm is lower than that on the undamaged beam after 127 days of sustained loading. The method offers an excellent controlling effect for the long-term performance of the strengthened damaged beams.

### 6.2.2. Under Negative Bending Moment

In engineering practice, components affected by negative bending moments are also typical. Since the damage occurs between the precast and post-cast parts, it is possible to examine whether this damage impacts the creep effect of strengthened components. Section 3.1 defines the component numbers, and Figure 19 depicts the test results.

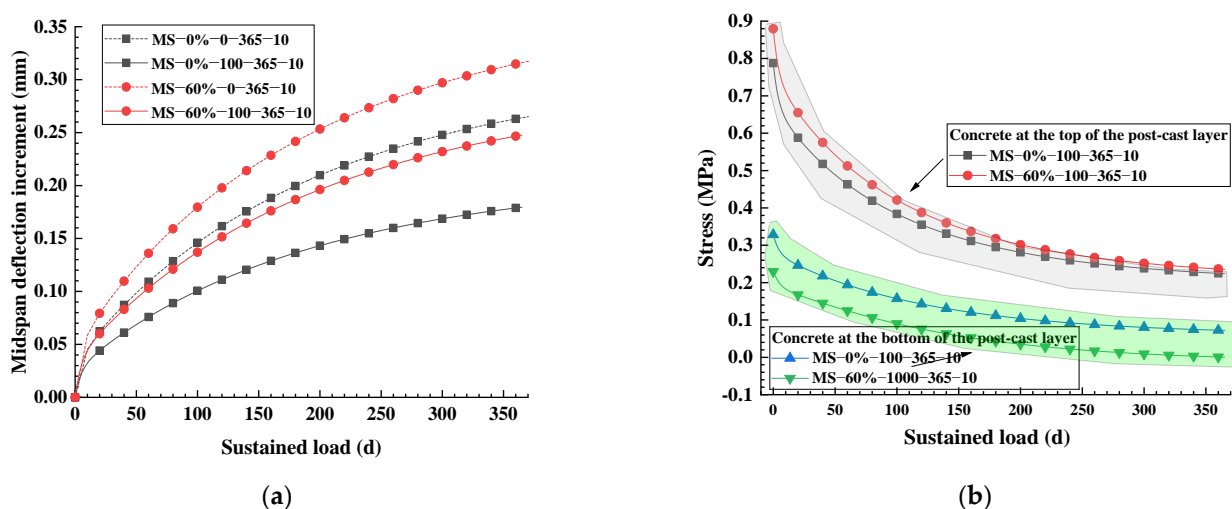


**Figure 19.** The creep of the concrete with different heights of reinforcement under a negative bending moment: (a) midspan deflection increment and (b) the section stress.

Figure 19a demonstrates that, under a negative bending moment, fatigue damage increases the midspan deflection of the beams compared with the undamaged beam under the effect of creep. After increasing the cross section, the deflection increment of the

damaged components declines to some extent, and the creep deflection increment of damaged component MS-60%-100-365-10 and undamaged component MS-0%-365-10-100 decreases by 21.6% and 32.0%, respectively, after 365 days of sustained loading. Therefore, increasing the cross section better controls the deflection of the damaged components under a negative bending moment.

## 7. Conclusions

The study presented in this paper established a simulation for the creep effect of fatigue-damaged concrete components and verified the validity of the model utilizing experimental data so as to analyze the creep of different damaged components under sustained loading. The following are the main conclusions drawn:

- On the basis of the principle of damage mechanics and strain equivalence, we established a creep structure of damaged concrete and proposed a numerical method for the creep effect of fatigue-damaged concrete components, which is suitable only for fatigue damage components but not for damage components, such as steel corrosion, concrete erosion, etc. The experimental results also validated the proposed model for the creep of damaged concrete components. The model could be used to forecast the creep deformation of undamaged components or damaged components after being strengthened, facilitating structural maintenance and decision-making about reinforcement.
- The mechanism for the influence of damage on the creep development of concrete beams was analyzed in conjunction with numerical calculations. The damage changed the stiffness of the cross section of the components and varied the stress state of the concrete in the cross section during loading, affecting the creep development of the concrete. Further, the creep of the components developed slowly as the age of the concrete increased.
- The undamaged beams were continuously loaded with 5 and 15 kN for 365 days, experiencing midspan deflections of 0.270 and 0.734 mm, respectively. When the load was elevated from 5 to 15 kN, the deflection enlarged by roughly 0.46 mm. The deflection of beam A-60%-100-365-10 and A-60%-100-3650-10 was 0.252 mm and 0.264 mm at the age of 365 and 3650 days, respectively. It increased by approximately 0.01 mm in 3285 days. Further, the stress magnitude had a more profound effect on the creep than the loading.
- The incremental creep deflection of the beams with a strengthened section height of 50, 100, and 150 mm loaded for 365 days decreased by 0.107, 0.228, and 0.326 mm, respectively, compared with the unstrengthened damaged beam. The method of reinforcing damaged beams with laminating post-cast part offered promising results in terms of controlling their creep deflection; in particular, increasing the section height had a profound effect. Moreover, this method excellently controlled the deflection of the damaged components under a negative bending moment.

## 8. Prospect

- This work investigated the impact of the creep of cracked concrete under low stress. For the nonlinear creep of damaged components at high stress levels, the initial damage to concrete may differ during the creep process. Thus, the nonlinear creep effect should be further investigated.
- This study focused on a single sort of damage, i.e., fatigue damage, and its influence on the creep effect of the component. However, in practice, multiple factors affect components' creep. Therefore, further research on creep is required under the combined impact of factors, such as material flaws, load, and the environment.

**Author Contributions:** Y.D., conceptualization, formal analysis, and writing—original draft; Y.F., data curation and visualization; W.J., supervision and funding acquisition; J.Z., investigation and project administration; B.L., writing—review and editing; J.M., methodology, writing—review and editing, and funding acquisition. All authors have read and agreed to the published version of the manuscript.

**Funding:** This work was supported by the National Natural Science Foundation of China (grant numbers 51820105012, 51878610); the Science and Technology Project of Sichuan Province (grant number 2022YFQ0048); and the Fundamental Research Funds for the Central Universities (grant number YJ2021130).

**Data Availability Statement:** All data, models, and code generated or used during this study are available upon request from the corresponding author.

**Conflicts of Interest:** The authors declare no conflict of interest.

## References

1. Chen, P.; Zhang, G.; Cao, S.; Lv, X.; Shen, B. Creep and post-creep mechanical properties of reinforced concrete columns. *J. Build. Eng.* **2023**, *63*, 105521. [CrossRef]
2. Abdelrahman, A. *Strengthening of Concrete Structures: Unified Design Approach, Numerical Examples and Case Studies*, 1st ed.; Springer Nature: Singapore, 2023; pp. 115–141.
3. Momayez, A.; Ehsani, M.; Rajaie, H.; Ramezani pour, A. Cylindrical specimen for measuring shrinkage in repaired concrete members. *Constr. Build. Mater.* **2005**, *19*, 107–116. [CrossRef]
4. Decter, M. Durable concrete repair—Importance of compatibility and low shrinkage. *Constr. Build. Mater.* **1997**, *11*, 267–273. [CrossRef]
5. Chen, X. An Experimental Research on the Differential Shrinkage and Creep of Simply Supported Rectangular Prestressed Concrete Composite Beams. *J. Wuhan Univ. Technol.* **1981**, *4*, 55–84.
6. Vassie, P.; TRRL. Reinforcement corrosion and the durability of concrete bridges. *Proc. Inst. Civ. Eng.* **1984**, *76*, 713–723. [CrossRef]
7. Wang, W.-W.; Weng, C.; Yang, W. Experimental Study on Creep and Shrinkage of Old and New Concrete Composite Beams. *J. Southeast Univ. (Nat. Sci. Ed.)* **2008**, *38*, 505–510.
8. Yang, W.; Xu, H. Practical Nonlinear Analysis Method of New-Old Concrete Composite Beams with Shrinkage and Creep. *Mech. Eng.* **2017**, *39*, 379–383. [CrossRef]
9. Guo, Y.-L.; Geng, Y.; Qu, L.-Y. Time-dependent behaviour of circular steel tube confined reinforced concrete (STCRC) stub columns subjected to low axial load. *Eng. Struct.* **2021**, *243*, 112663. [CrossRef]
10. Gilbert, R.I. Time-Dependent Analysis of Composite Steel-Concrete Sections. *J. Struct. Eng.* **1989**, *115*, 2687–2705. [CrossRef]
11. Ayoub, A.; Filippou, F.C. Mixed Formulation of Nonlinear Steel-Concrete Composite Beam Element. *J. Struct. Eng.* **2000**, *126*, 371–381. [CrossRef]
12. Nguyen, Q.-H.; Hjjaj, M. Nonlinear Time-Dependent Behavior of Composite Steel-Concrete Beams. *J. Struct. Eng.* **2016**, *142*, 04015175. [CrossRef]
13. Fang, Y.; Mao, J.; Zhang, Y.; Jin, W.; Tang, D.; Zhang, J. Calculation of Deflection and Stress of Assembled Concrete Composite Beams under Shrinkage and Creep and Its Application in Member Design Optimization. *KSCE J. Civ. Eng.* **2021**, *25*, 3458–3476. [CrossRef]
14. Henriques, D.; Gonçalves, R.; Sousa, C.; Camotim, D. GBT-based time-dependent analysis of steel-concrete composite beams including shear lag and concrete cracking effects. *Thin-Walled Struct.* **2020**, *150*, 106706. [CrossRef]
15. Ferrier, E.; Hamelin, P. Durability of Reinforced Concrete Beams Repaired by Composites under Creep and Fatigue Loading. In *Recent Developments in Durability Analysis of Composite Systems*, 1st ed.; CRC Press: London, UK, 2000; pp. 279–289. Available online: <https://www.taylorfrancis.com/chapters/edit/10.1201/9781003211181-37/durability-reinforced-concrete-beams-repaired-composites-creep-fatigue-loading-ferrier-hamelin> (accessed on 1 April 2023).
16. Farah, M.; Grondin, F.; Alam, S.; Loukili, A. Experimental approach to investigate creep-damage bilateral effects in concrete at early age. *Cem. Concr. Compos.* **2019**, *96*, 128–137. [CrossRef]
17. Cao, G.-H.; Han, C.-C.; Peng, P.; Zhang, W.; Tang, H. Creep Test and Analysis of Concrete Columns under Corrosion and Load Coupling. *ACI Struct. J.* **2019**, *116*, 121–130. [CrossRef]
18. Zhou, H.Y.; Chen, Y.B.; Ci, J.C.; Yang, C.K. Research Status of Fatigue Damage Mechanism of Reinforced Concrete Beam. *Sci. Net* **2017**, *858*, 44–49. Available online: <https://www.scientific.net/amm.858.44> (accessed on 1 April 2023). [CrossRef]
19. Kachanov, L.M.; Krajcinovic, D. Introduction to Continuum Damage Mechanics. *J. Appl. Mech.-Trans. Asme-J. Appl. Mech.* **1987**, *54*, 481. [CrossRef]
20. Zhang, T.; McHugh, P.; Leen, S. Finite element implementation of multiaxial continuum damage mechanics for plain and fretting fatigue. *Int. J. Fatigue* **2012**, *44*, 260–272. [CrossRef]
21. Van Do, V.N.; Lee, C.-H.; Chang, K.-H. High cycle fatigue analysis in presence of residual stresses by using a continuum damage mechanics model. *Int. J. Fatigue* **2015**, *70*, 51–62. [CrossRef]

22. Bazant, Z.P. Discussion of L. F. Nielsen's paper "On the applicability of modified dischinger equations". *Cem. Concr. Res.* **1978**, *8*, 117–119. [[CrossRef](#)]
23. Du, J.; Mao, C.; Si, T. *Bridge Structure Analysis*, 1st ed.; Tongji University Publishing: Shanghai, China, 1994; pp. 32–38.
24. Xiao, R. *Bridge Structure Analysis and Program System*, 1st ed.; People's Communications University Press: Beijing, China, 2002; pp. 10–17.
25. Lemaitre, J. How to use damage mechanics. *Nucl. Eng. Des.* **1984**, *80*, 233–245. [[CrossRef](#)]
26. Mai, S.; Le-Corre, F.; Foret, G.; Nedjar, B. A continuum damage modeling of quasi-static fatigue strength of plain concrete. *Int. J. Fatigue* **2012**, *37*, 79–85. [[CrossRef](#)]
27. Zhu, B. An Implicit Method for the Stress Analysis of Concrete Structures Considering the Effect of Creep. *J. Hydraul. Eng.* **1983**, *5*, 40–46. Available online: [http://en.cnki.com.cn/Article\\_en/CJFDTOTAL-SLXB198305004.htm](http://en.cnki.com.cn/Article_en/CJFDTOTAL-SLXB198305004.htm) (accessed on 1 April 2023).
28. Zhan, Z.; Meng, Q.; Hu, W.; Sun, Y.; Shen, F.; Zhang, Y. Continuum damage mechanics based approach to study the effects of the scarf angle, surface friction and clamping force over the fatigue life of scarf bolted joints. *Int. J. Fatigue* **2017**, *102*, 59–78. [[CrossRef](#)]
29. Boumakis, I.; Ninčević, K.; Marcon, M.; Vorel, J.; Wan-Wendner, R. Bond stress distribution in adhesive anchor systems: Interplay of concrete and mortar creep. *Eng. Struct.* **2021**, *250*, 113293. [[CrossRef](#)]
30. Zhu, B. *Temperature Stress and Temperature Control of Hydraulic Concrete Structures*, 1st ed.; Water Resources and Electric Power Press: Beijing, China, 1976; pp. 137–184.
31. GB50010-2010; Code for Design of Concrete Structures. China Architecture and Building Press: Beijing, China, 2010.
32. Fan, Z.; Sun, Y. Detecting and evaluation of fatigue damage in concrete with industrial computed tomography technology. *Constr. Build. Mater.* **2019**, *223*, 794–805. [[CrossRef](#)]
33. Pan, H.; Qiu, H.X. Numerical Simulation of Fatigue Performance of Reinforced Concrete Flexural Components. *J. Southeast Univ. (Nat. Sci. Ed.)* **2006**, *6*, 997–1001. Available online: [http://en.cnki.com.cn/Article\\_en/CJFDTOTAL--DNDX200606024.htm](http://en.cnki.com.cn/Article_en/CJFDTOTAL--DNDX200606024.htm) (accessed on 4 March 2023).
34. Isleem, H.F.; Augustino, D.S.; Mohammed, A.S.; Najemalden, A.M.; Jagadesh, P.; Qaidi, S.; Sabri, M.M.S. Finite element, analytical, artificial neural network models for carbon fibre reinforced polymer confined concrete filled steel columns with elliptical cross sections. *Front. Mater.* **2023**, *9*, 1115394. [[CrossRef](#)]
35. Hawileh, R.; Nawaz, W.; Abdalla, J.; Saqan, E. Effect of flexural CFRP sheets on shear resistance of reinforced concrete beams. *Compos. Struct.* **2015**, *122*, 468–476. [[CrossRef](#)]
36. Kim, Y.J.; Harries, K.A. Fatigue behavior of damaged steel beams repaired with CFRP strips. *Eng. Struct.* **2011**, *33*, 1491–1502. [[CrossRef](#)]
37. GB 503672013; Code for Design of Reinforcement of Concrete Structures. China Industry Press: Beijing, China, 2013.
38. Isleem, H.F.; Jagadesh, P.; Qaidi, S.; Althoey, F.; Rahmawati, C.; Najm, H.M.; Sabri, M.M.S. Finite element and theoretical investigations on PVC-CFRP confined concrete columns under axial compression. *Front. Mater.* **2022**, *9*, 1055397. [[CrossRef](#)]
39. Li, L.; Guo, Y.; Liu, F.; Bungey, J. An experimental and numerical study of the effect of thickness and length of CFRP on performance of repaired reinforced concrete beams. *Constr. Build. Mater.* **2006**, *20*, 901–909. [[CrossRef](#)]
40. Ying, J.; Guo, J. Fracture Behaviour of Real Coarse Aggregate Distributed Concrete under Uniaxial Compressive Load Based on Cohesive Zone Model. *Materials* **2021**, *14*, 4314. [[CrossRef](#)] [[PubMed](#)]
41. Tang, D.; Jin, W.; Mao, J.; Zhao, Y. Influence of Shrinkage and Creep on Deflections of Assembled Concrete Composite Beams. *J. Civ. Environ. Eng.* **2019**, *41*, 127–134, (In English and Chinese).
42. Ma, Z.; Shen, J.; Wang, C.; Wu, H. Characterization of sustainable mortar containing high-quality recycled manufactured sand crushed from recycled coarse aggregate. *Cem. Concr. Compos.* **2022**, *132*, 104629. [[CrossRef](#)]
43. Cagnon, H.; Vidal, T.; Sellier, A.; Bourbon, X.; Camps, G. Drying creep in cyclic humidity conditions. *Cem. Concr. Res.* **2015**, *76*, 91–97. [[CrossRef](#)]
44. Huixiang, M.; Zhigang, L.; Zhang, Y.; Haoran, X. Research on the Bearing Capacity of the Cross Section of Reinforced Concrete Beams Strengthened with Increasing Section Method Considering the Effect of the Second Loading. *Adv. Res.* **2015**, *5*, 1–9. [[CrossRef](#)]
45. Hui, R.; Huang, G.; Yi, R. *Shrinkage Creep*, 1st ed.; China Railway Press: Beijing, China, 1988; pp. 236–312.
46. Liu, Z.; Zheng, X. An Analysis of the Section-Enlarging Reinforcing Method for Concrete. *Traffic Eng. Technol. Natl. Def.* **2006**, *4*, 68–70. Available online: [http://en.cnki.com.cn/Article\\_en/CJFDTOTAL-GFJT200604021.htm](http://en.cnki.com.cn/Article_en/CJFDTOTAL-GFJT200604021.htm) (accessed on 1 April 2023).

**Disclaimer/Publisher's Note:** The statements, opinions and data contained in all publications are solely those of the individual author(s) and contributor(s) and not of MDPI and/or the editor(s). MDPI and/or the editor(s) disclaim responsibility for any injury to people or property resulting from any ideas, methods, instructions or products referred to in the content.